Paper

Fusion Splicing and Testing of Photonic Crystal Fibers

Krzysztof Borzycki

Abstract—Properties of two different photonic crystal fibers (PCF) were characterized, enabling comparisons. Properties investigated included spectral attenuation, polarization mode dispersion (PMD), optical time domain reflectometer characteristics, elastooptic factor describing transmission delay induced by axial strain plus effects of temperature cycling and fiber twist on PMD and loss. In particular, temperature and twist dependence of PMD was different for each fiber tested. For optical measurements, fibers were fusion spliced to pigtails with standard telecom single mode fibers. PCF splicing procedures and solutions adopted to minimize collapse of holes during arc fusion and splice loss are presented. It was found that fusion splicing procedure must be individually tailored to each combination of fibers.

Keywords—fusion splicing, measurements, mechanical testing, photonic crystal fiber, polarization mode dispersion, temperature cycling.

1. Introduction

Experiments presented in this paper have been carried out at the laboratories of National Institute of Telecommunications (NIT) in Warsaw as part of participation in the COST Action 299 "Optical Fibres for New Challenges Facing the Information Society" (FIDES)[1], dedicated to new applications of fiber optics. This includes research and characterization work on new fiber designs, in particular highly-doped and photonic crystal fibers.

Photonic crystal fibers with germanium-doped core, designated as 252b5 and 282b4 were provided by Institute of Photonic Technology (IPHT) Jena, Germany – another participant of COST-299.

Besides characterization of each photonic crystal fibers (PCF), another goal of work was to research fusion splicing of PCF to standard single mode fibers (SMF). Most fiber optic measuring instruments are designed specifically to test SMF and similar solid-glass fibers, so a convenient way to prepare sample of specialty fiber for measurements is to splice it to SMF pigtails with connectors of choice. As low splice loss and stability of loss and polarization orientation are highly desirable, a proven fusion splicing method is preferred. This is of particular importance during temperature cycling and mechanical experiments.

Earlier work at NIT within COST-299 on PCF characterization, including IPHT 252b5 has been reported in 2008 [1]. Some data from this paper are included here for comparisons.

[1]More information on this COST Action can be found at www.cost299.org

2. The Fibers

Both PCF were designed to be single mode at wavelengths above 1300 nm, made of silica, and had a small core doped with GeO_2, with a wider "base" and central "peak", surrounded by a multilayer array of holes. Fibers had thin, mechanically strippable, single-layer acrylate coating. Fiber data are listed in Table 1.

Table 1
Fiber data supplied by IPHT

Parameter	IPHT 252b5	IPHT 282b4
Cladding diameter [μm]	82.7	124.4
Number of holes	90	94
Hole diameter (d) [μm]	3.6	~0.7
Hole spacing (Λ) [μm]	4.2	4.2
Diameter of holey package [μm]	42.8	43.0
Cross-section occupied by holes [%]	17.1	0.3
Cladding diameter after collapse [μm]	75.3	124.2
Core diameter [μm]	0.5/2.0/4.1	1.2/3.9/7.3

Both fibers had relatively small cores and high doping levels in comparison to SMF used in communication networks, where typical core diameter is 7–9 μm [2], [3]. This applies in particular to IPHT 252b5, designed as highly nonlinear PCF for applications like optical signal processing. This property leads to considerable difficulties in making low-loss splices between PCF and SMF.

Hole diameters listed in Table 1 were measured with optical microscope; scanning electron microscope (SEM) observations at IPHT found that hole diameters in 282b4 vary considerably, down to about 0.5 μm.

3. Fusion Splicing

3.1. Connections to Test Instruments

For connection to test instruments each PCF was fusion spliced to pigtails with SMF fibers, most often Corning SMF-28 or OFS MC-SM, 2–3 m long and terminated with FC/PC connectors (Fig. 1). For optical time domain reflectometer (OTDR) measurements, SMF lengths must be increased to $\geq$ 100 m in order to eliminate the dead zone.

Splices were protected by standard 60 mm heat shrinkable sleeves reinforced with steel rods, being often subjected to thermal cycling or used to fix ends of PCF during mechan-

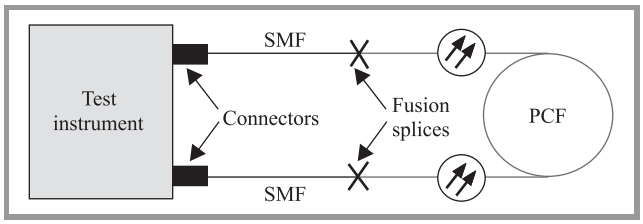

Fig. 1. Connection of PCF sample to measuring instrument.

ical tests. Because of differences between fibers, splicing procedure had to be adjusted individually.
In line with prior experience [1], no solvent was used in preparations for PCF cleaving; the coating was stripped mechanically and remains wiped away with dry tissue. A standard cleaver with tungsten carbide blade was used. Proportion of bad cleaves was significant for 252b5 fiber, while the 282b4 handled comparably to 125 μm telecom fibers. Fiber positioning before splicing was optimized using optical source and power meter. For most measurements an HP8153A optical multimeter with HP8153SM 1558 nm laser source and HP81532A power meter modules was used.
When splicing SMF to PCF, often of different diameter, three problems arise:

a) thinner fiber must receive less power to prevent overheating;

b) collapse of holes in the PCF tends to increase splice loss and shall be controlled;

c) sharp edges must be avoided to ensure splice strength.

A solution to problem (a) is to offset the fiber contact point from the axis of electrodes, so the smaller fiber is kept away from center of discharge zone and is heated less. This longitudinal offset shall not be greater than (1.5–2) $\times$ the diameter of thicker fiber; larger offset can lead to fiber deformation.
Collapse of holes in PCF is hard to avoid, but length affected is minimized by short fusion time, preferably 0.2–0.5 s, instead of 1–2 s common in splicing of conventional 125 μm single mode and multimode fibers. Careful control of arc power is essential. Unfortunately, too short fusion time and low arc power prevent proper rounding of edges when fiber diameters don't match, as molten glass does not have enough time to flow. This leads to fragile splices which break easily.
Loss of fusion splice between fibers of different core sizes and designs can be reduced by:

– insertion of a short piece of fiber with intermediate core parameters [4];

– individually optimized forming of fibers before fusion; examples include pulling hot fiber to reduce diameter before cleaving, thermal expansion of core by heat treatment and melting of PCF tip to close the holes over controlled length and expand light beam, or to create a ball lens [5].

The following sections describe experiences with splicing of PCF and SMF fibers.

3.2. Splicing IPHT 252b5 to SMF

Out of methods listed above, fusing of SMF and PCF tips into lenses [5] was of particular interest. It was applied at NIT to splice a sample of thin, small-core IPHT 252b5 fiber (Table 1) to Corning SMF-28 single mode fibers. Previous attempts [1], when SMF and PCF were butt-coupled with 150 μm offset during fusion produced splices with good strength, but loss of SMF-PCF-SMF assembly with 1 m of PCF was high: 16.8 dB at 1550 nm.
Splicing of IPHT 252b5 sample to SMF-28 pigtails is presented below, including photos taken through the microscope of fusion splicer and loss measurements at 1558 nm. The PCF sample was 16.08 m long; fiber attenuation and loss were 114 dB/km and 1.83 dB, respectively, at 1558 nm. Fusion splicer had 1 mm electrode gap, and the following settings (arc current – duration) were adopted:

– splicing (pre-fusion, fusion, annealing):
9 mA – 3.0 s / 18 mA – 0.5 s / 8.4 mA – 3.0 s;

– melting of fiber tip: 18 mA – 0.5 s.

Fiber feed during fusion was approx. 20 μm. Splicing standard SMF with the same machine requires 18–19 mA fusion current and 1.2 – 1.5 s fusion duration.

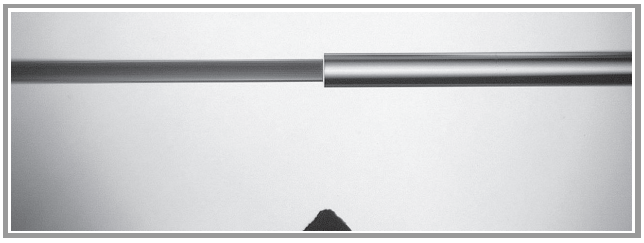

Fig. 2. Fibers cleaved and aligned with 10 μm gap (loss: 8.18 dB, electrode tip visible at the bottom).

Fig. 3. SMF tip melted into a ball: (a) phase 1; (b) phase 2.

Work began with connecting the first pigtail to a 1558 nm laser source. The opposite end of PCF was cleaved and connected to optical power meter. Figures 2–10 show making of the first splice, where light traveled from SMF to PCF. Field of view in all splicer photos is 0.88×2.35 mm. After cleaving and measuring reference loss (Fig. 2), fibers were melted to make ball lenses at their ends (Figs. 3–5). Melting of SMF tip had to be repeated for proper effect (Fig. 3).

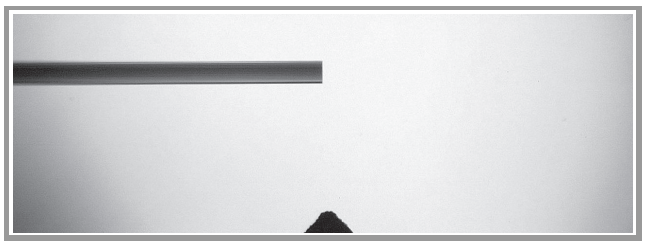

Fig. 4. PCF tip positioned for ball forming.

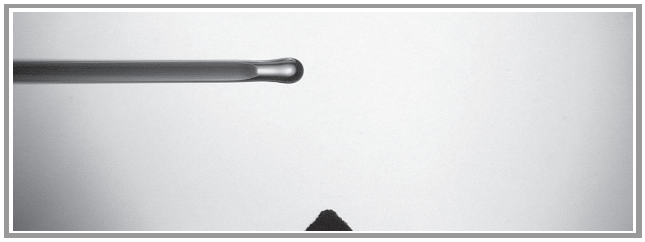

Fig. 5. PCF tip melted into a ball. Holes collapsed over 180–200 μm length.

Radii of ball lenses were 48 μm for PCF and 74 μm for SMF. Prepared fibers were positioned for best coupling, with longitudinal offset to reduce PCF heating during fusion (Fig. 6), than fused (Fig. 7).

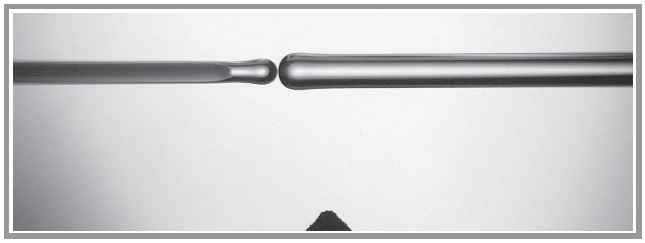

Fig. 6. Lens-tipped fibers positioned with ≈ 10 μm gap (offset: 200 μm, loss: 5.48 dB).

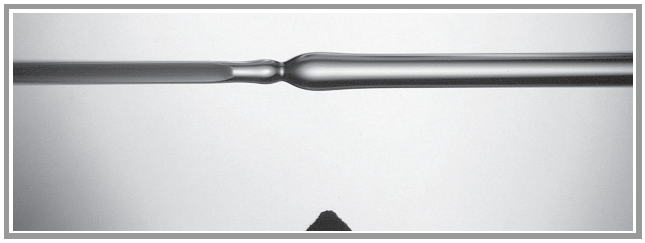

Fig. 7. PCF and SMF spliced (loss: 3.76 dB).

After fusion, attempts were made to reduce splice loss with additional heating, by repeating fusion program without moving fibers. It worked, but with diminishing effect (Figs. 8–10).

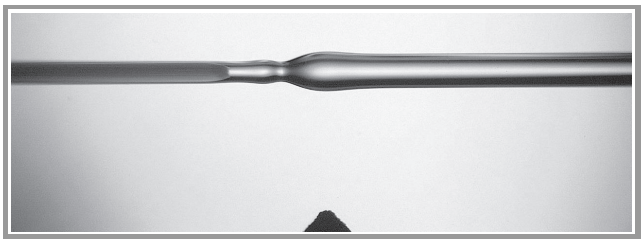

Fig. 8. PCF and SMF after additional heating no. 1 (loss: 3.43 dB).

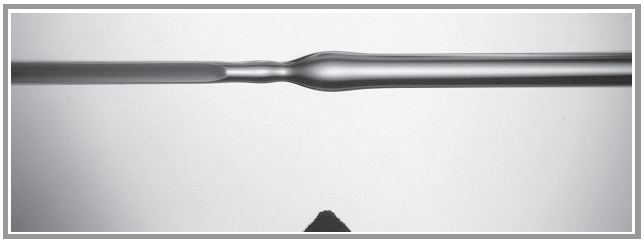

Fig. 9. PCF and SMF after additional heating no. 2 (loss: 3.24 dB).

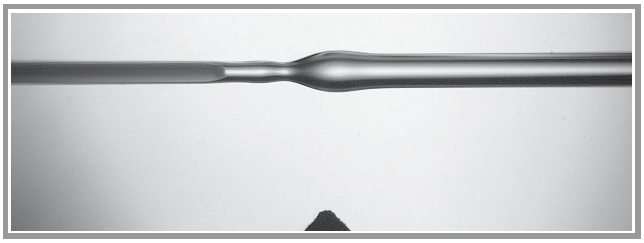

Fig. 10. PCF and SMF after additional heating no. 3 (loss: 3.19 dB).

Table 2
Loss of IPHT 252b5 sample during splicing to SMF pigtails

Conditions	Sample loss [dB]	Splice loss [dB]
SMF → PCF splice (first)		
Fibers cleaved and aligned	8.18	6.15
Lens-tipped fibers aligned	5.48	3.45
Fibers spliced	3.76	1.73
After heating no. 1	3.43	1.40
After heating no. 2	3.24	1.21
After heating no. 3	3.19	1.16
PCF → SMF splice (second)		
Fibers cleaved and aligned	8.98	5.79
Lens-tipped fibers aligned	5.37	2.18
Fibers spliced	4.61	1.42
After heating no. 1	4.38	1.19
After heating no. 2	4.28	1.09
After heating no. 3	4.17	0.98

The second splice transmitted light from PCF to SMF. For loss measurement, the second pigtail was connected to power meter. Loss values in various stages of splicing at both ends are listed in Table 2.
Subtracting 0.20 dB for connector loss and 1.83 dB for PCF loss, we get 2.14 dB for two splices. Transfer of light

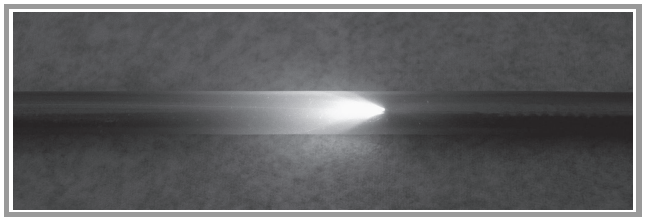

Fig. 11. Escape of visible light in transit from SMF (right) to IPHT 252b5 (left). Splice inside a heat-shrinkable sleeve filled with opaque hot melt glue. Illumination with supercontinuum (SC) source.

from SMF to PCF causes majority of loss: 1.16 dB, due to escape of radiation from the splice (Fig. 11).

3.3. Splicing IPHT 282b4 to SMF

This PCF was spliced without longitudinal offset (Fig. 12), using 17 mA fusion current and other conditions as in Subsection 3.2. Fiber length, attenuation and loss at 1558 nm were 12.4 m, 62 dB/km and 0.77 dB, respectively. After

Fig. 12. SMF (right) and IPHT 282b4 (left) cleaved and aligned with ≈ 10 μm gap.

Fig. 13. SMF and IPHT 282b4 fused.

fusion, holes collapsed over 280–300 μm (Fig. 13), but loss still fell in comparison to cleaved and aligned fibers, regardless of transmission direction.

Loss values at 1558 nm are listed in Table 3. Assuming 0.25 dB connector loss, the loss of two splices is 2.74 dB.

Table 3
Loss of IPHT 282b4 sample during splicing to SMF pigtails

Conditions	Sample loss [dB]	Splice loss [dB]
SMF → PCF splice (first)		
Fibers cleaved and aligned	3.73	2.71
Fibers spliced	2.50	1.48
Protective sleeve applied	2.52	1.50
PCF → SMF splice (second)		
Fibers cleaved and aligned	4.79	2.27
Fibers spliced	3.77	1.25
Protective sleeve applied	3.76	1.24

Loss in each direction of transmission is similar, as can be expected when core diameters of spliced fibers are comparable (Table 1). Part of splice loss is likely due to destruction of holey structure and escape of light. One can expect improvement when PCF heating is reduced by offset or lower arc current.

4. Spectral Loss

Loss spectra of two pigtailed IPHT 252b5 samples were acquired with supercontinuum light source Koheras SuperK Compact and optical spectrum analyzer Yokogawa AQ-6315B.

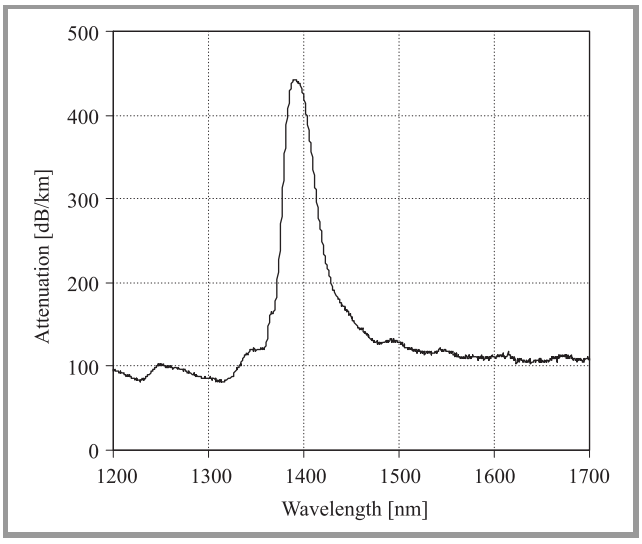

Fig. 14. Spectral attenuation of IPHT 252b5 fiber.

Characteristics of IPHT 252b5 fiber, shown in Fig. 14 and Table 4 was established by comparing loss spectra of two lengths: 0.50 m and 16.08 m, spliced in the same way

to SMF pigtails. Attenuation can be attributed to waveguide imperfections (80–105 dB/km) and OH^- ion absorption ($\sim$ 355 dB/km at 1390 nm); the latter corresponds to water

Table 4
Attenuation of IPHT 252b5 fiber
at selected wavelengths

Wavelength [nm]	Attenuation [dB/km]
1200	95
1248	103
1315	82
1390	443
1550	119
1700	110

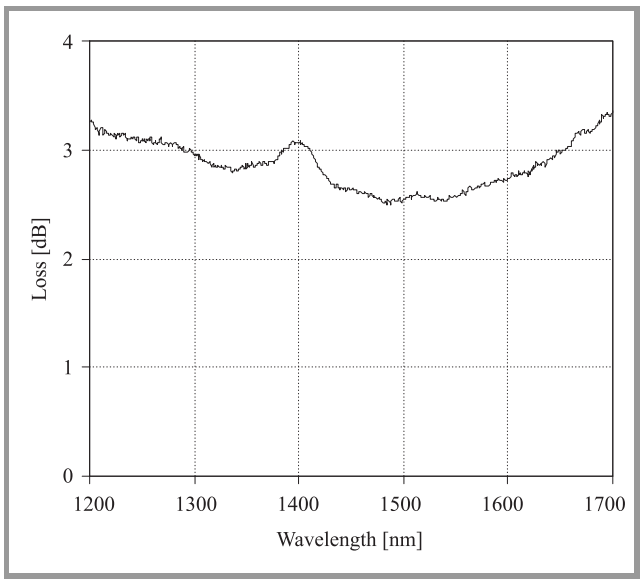

Fig. 15. Loss spectrum of 0.5 m sample of IPHT 252b5 with SMF pigtails.

content of about 7 ppm. Loss spectrum of the 0.50 m sample (Fig. 15) is pretty flat, with minimum splice loss at 1500 nm.

5. OTDR Measurements

Sample of 282b4 fiber was measured using Tektronix TFP2 OTDR fitted with FS 1315 optical module. The 252b5 sample available was too short for this purpose.

This PCF was characterized by very strong Rayleigh backscattering. Its OTDR trace (Fig. 16) was shifted upwards by approx. 9 dB with respect to trace of SMF (OFS MC-SM [3]) at wavelengths of 1310 nm and 1550 nm, when loss of splice and connector between SMF and PCF (0.5 dB) was corrected for. This means an 80-fold difference in backscatter power. Possibly, the photonic

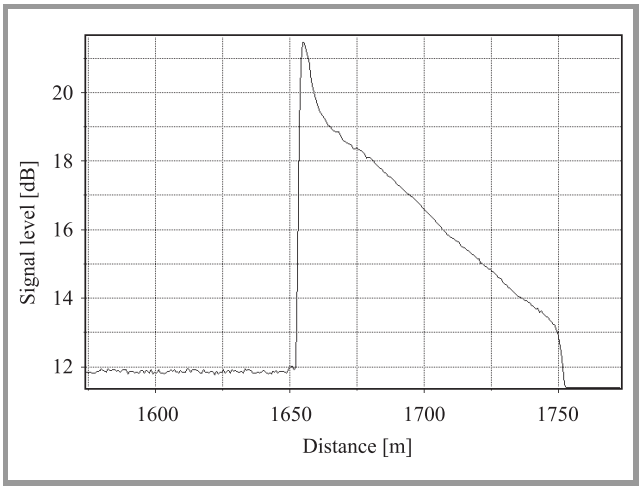

Fig. 16. OTDR trace of 104 m IPHT 282b4 preceded by 1645 m long SMF, $\lambda = 1310$ nm. Reflection spike is due to connector located between SMF and PCF.

structure around PCF core reflects scattered light back into the core. Backscattering coefficients are approx. –71 dB and –73 dB for a 1 m pulse at 1310 nm and 1550 nm, respectively.

Table 5
OTDR test results – IPHT 282b4

Parameter	Value
Fiber attenuation at 1310 nm [dB/km]	69.3
Fiber attenuation at 1550 nm [dB/km]	60.2
Trace shift versus MC-SM at 1310 nm [dB]	8.7
Trace shift versus MC-SM at 1550 nm [dB]	9.5

Optical time domain reflectometer traces were quite linear, with deviations within ± 0.2 dB. Loss values measured with OTDR were confirmed by measurement with laser source and optical power meter. Results are shown in Table 5.

6. Polarization Mode Dispersion

Measurements were made at room temperature with Adaptif Photonics A2000 PMD analyzer and Agilent HP8168F

Table 6
Results of PMD and polarization
dependent loss (PDL) measurements

Fiber	Length [m]	PMD [ps]	PMD coefficient [ps/km]	PDL [dB]
IPHT 252b5	0.50	0.547	1094	0.23
IPHT 252b5	16.08	18.120	1127	0.15
IPHT 282b4	12.40	1.455	117.34	0.37
IPHT 282b4	104	9.104	87.54	0.03

tunable laser in the 1460–1590 nm band, using the Jones matrix eigenalysis (JME) method. Two different lengths of each fiber cut were from the same delivery length. Results are listed in Table 6. Differential group delay (DGD) spectra are shown in Figs. 17 and 18. PCF length uncertainty was 2%.

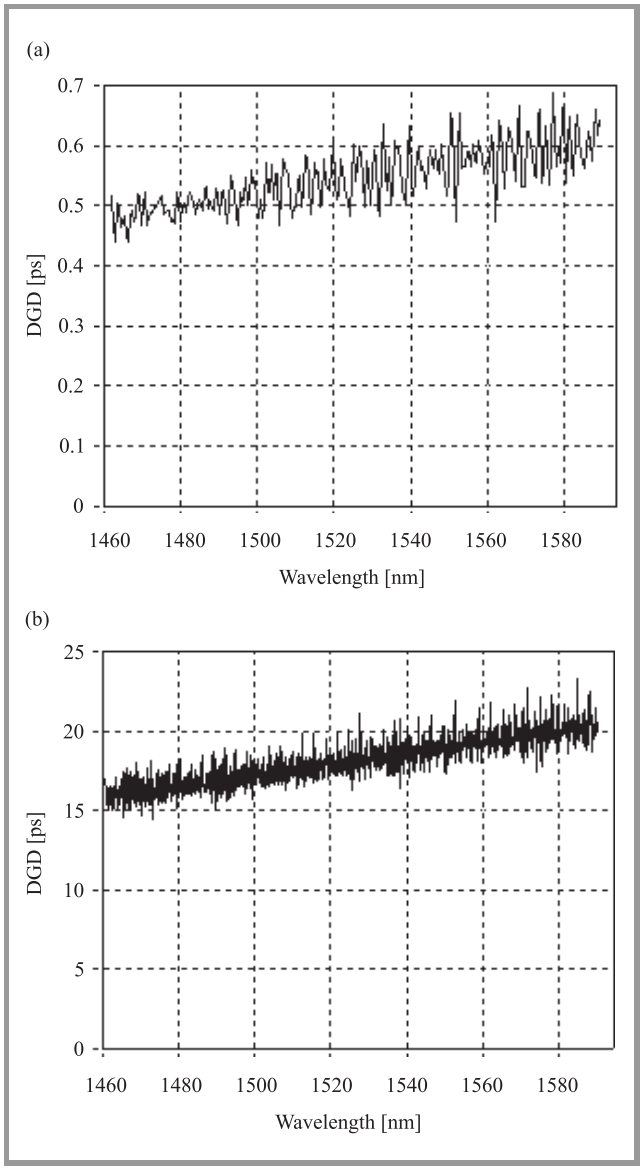

Fig. 17. DGD spectra of IPHT 252b5 fiber: (a) $L = 0.50$ m; (b) $L = 16.08$ m.

The IPHT 252b5 fiber exhibited very high PMD coefficient and linear increase of DGD with wavelength, identical for both lengths tested.

Differential group delay distribution of IPHT 282b4 was flat with some random deviations. A lower PMD coefficient in the longer sample suggests some mixing of polarization modes, confirmed by somewhat irregular movement of state of polarization on Poincare sphere with wavelength. For the shorter sample of IPHT 282b4 and both lengths of 252b5 a circular movement was observed.

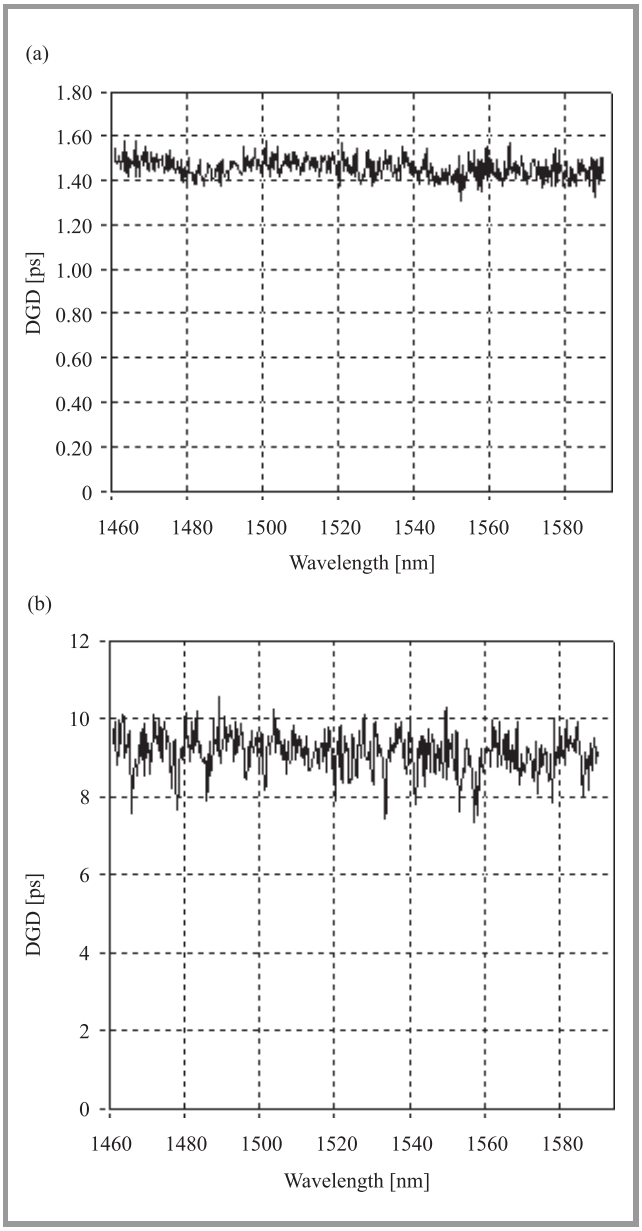

Fig. 18. DGD spectra of IPHT 282b4 fiber: (a) $L = 12.40$ m; (b) $L = 104$ m.

7. Temperature Cycling

Each fiber was subjected to a single temperature cycle with measurements of polarization parameters and loss, using Adaptif Photonics A2000 PMD analyzer and Agilent HP8168F tunable laser.

To minimize external forces acting on fiber under test, the short sample of IPHT 252b5 was loosely placed on a flat plate, while IPHT 282b4 was wound on a 160 mm diameter spool with soft foam bedding. Whole length of PCF and both PCF-SMF splices were placed inside the environmental chamber. Measurements at reference temperature (+20°C) were performed twice to detect any permanent change in fiber parameters, e.g., due to deterioration of protective coating.

Results are shown in Tables 7 and 8, and Figs. 19 and 20. PMD, PDL and insertion loss data are averages for the whole spectral range. Sample of IPHT 252b5 was spliced using old non-optimized method [1].

Table 7
IPHT 252b5 – temperature cycling test
(fiber length 1.02 m; $\lambda = 1480$–1550 nm)

Temperature [°C]	PMD [ps]	PMD coefficient [ps/km]	Relative PMD	PDL [dB]	Loss [dB]
+20	1.104	1082.4	1.0000	0.44	17.97
–20	1.100	1078.4	0.9964	0.46	17.92
0	1.102	1080.4	0.9982	0.42	17.93
+20	1.104	1082.4	1.0000	0.45	17.96
+40	1.106	1084.3	1.0018	0.45	17.96
+60	1.107	1085.3	1.0027	0.52	17.96

Table 8
IPHT 282b4 – temperature cycling test
(fiber length 12.40 m; $\lambda = 1490$–1590 nm)

Temperature [°C]	PMD [ps]	PMD coefficient [ps/km]	Relative PMD	PDL [dB]	Loss [dB]
+20	1.456	117.45	1.000	0.03	4.21
–30	1.538	124.03	1.056	0.03	4.21
–10	1.502	121.13	1.032	0.03	4.21
+10	1.474	118.87	1.012	0.03	4.21
+30	1.445	116.49	0.992	0.03	4.21
+50	1.419	114.44	0.975	0.03	4.21
+70	1.393	112.34	0.957	0.03	4.22
+20	1.466	118.23	1.007	0.03	4.21

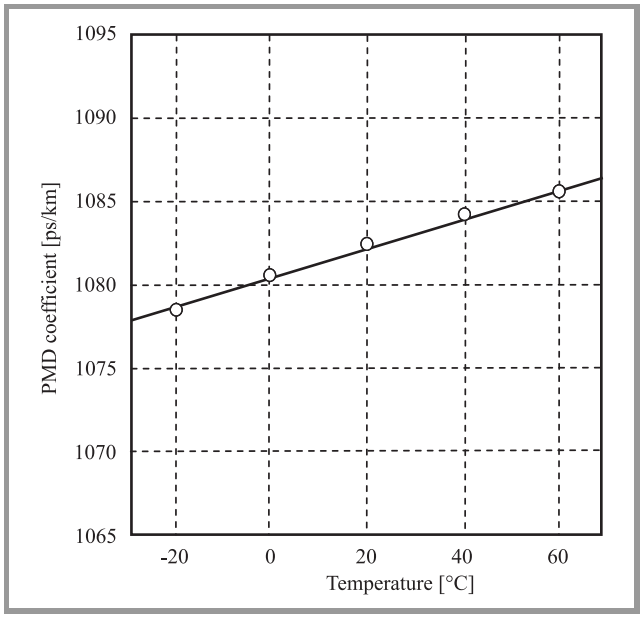

Fig. 19. Temperature characteristics of PMD – IPHT 252b5.

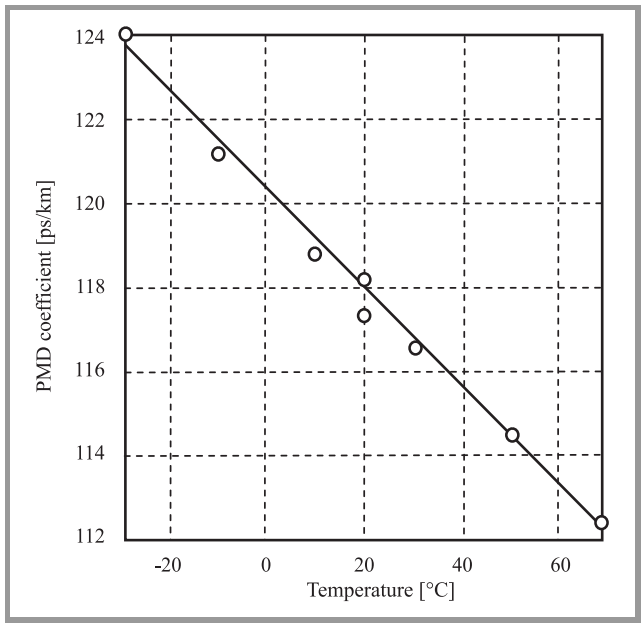

Fig. 20. Temperature characteristics of PMD – IPHT 282b4.

Temperature coefficients of PMD were $+7.9 \cdot 10^{-5}$/K for IPHT 252b5 and $-9.7 \cdot 10^{-4}$/K for IPHT 282b4.

Temperature dependence of PMD in IPHT 282b4 is similar to PANDA fibers, where birefringence is produced by strain generated by mismatch in thermal expansion of fiber parts. This effect is characterized by fictive zero-strain temperature of approximately +1100°C and negative temperature coefficient of about $-9 \cdot 10^{-4}$/K, matching the test data. Low and positive temperature coefficient of PMD in IPHT 252b5 indicates that its PMD is not resulting from mechanical strain, but non-symmetrical geometry of fiber core and surrounding holey structure.

Both samples exhibited excellent stability of loss with temperature. This applies also to fusion splices, exposed to variable temperatures during tests. Permanent changes of fiber attenuation and PMD due to temperature cycling are within measurement uncertainty.

8. PMD Versus Fiber Twist

8.1. Test Procedure and Results

Twisting of fiber reduces its PMD, as the circular strain causes periodic rotation of polarization states and prevents accumulation of differential group delay along the fiber. This applies both to PMD resulting from non-symmetry of fiber core [6], and PMD induced by external forces acting on the fiber [7]. However, circular strain also produces PMD proportional to twist rate, so progressive twisting causes PMD to drop first – when initial fiber birefringence is reduced, but increase later [6].

Experimental investigation of this effect in PCF is easier than in telecom single mode fibers, because many PCFs have high PMD coefficients and short sample is sufficient. Earlier twisting tests on PCF [8] gave PMD versus twist characteristics similar to conventional fibers.

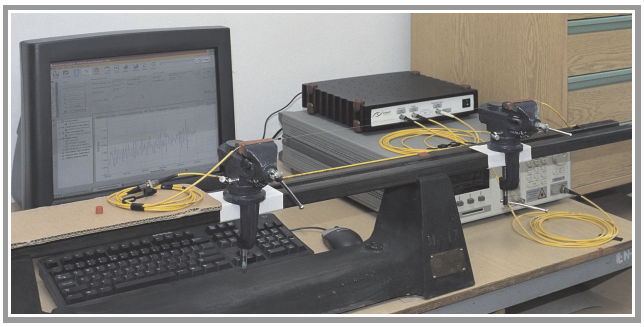

Fig. 21. Twist test of IPHT 252b5 (twisted length 0.50 m). PMD analyzer (Adaptif Photonics A2000), PC and tunable laser source (HP8168F) visible in the background.

A straight sample of each PCF was suspended between supports (Fig. 21) by gripping splice protection sleeves. One end of PCF was fixed, while the other was rotated as required. To avoid twisting of pigtails and interconnecting fibers, the sample was disconnected each time the movable end was to be rotated and re-connected before measurement.

Increase of PMD after initial reduction was not observed in both fibers till the maximum twist rate applied. Figures 22 and 23 are plots of relative PMD versus twist rate.

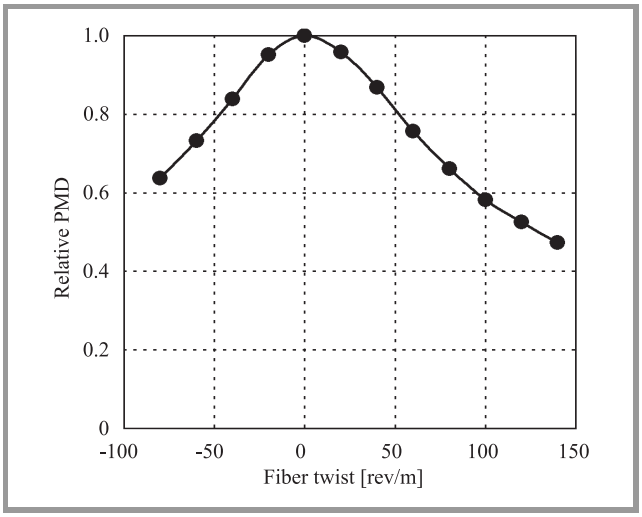

Fig. 22. PMD versus twist rate – IPHT 252b5. Twisting in two directions.

Lesiak and Woliński [9] reported only a small ($\leq 0.7\%$) decrease of PMD in two PCF samples twisted up to 40 rev/m. The fibers tested had PMD coefficients comparable to IPHT 252b5: 2300 ps/km and 730 ps/km, but lacked fully symmetric holey package, as one row of holes near the core

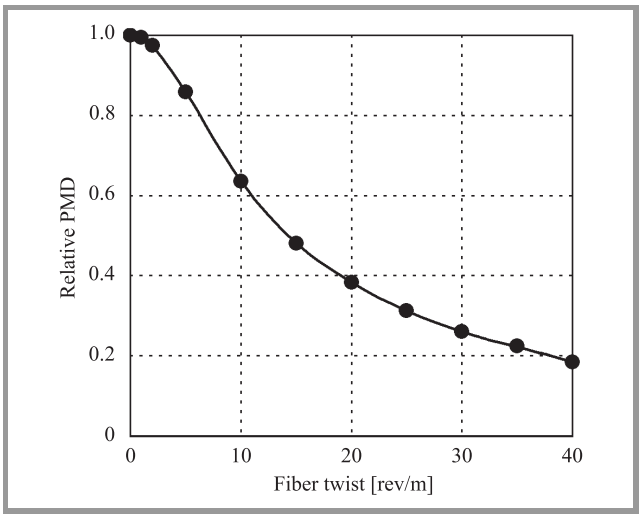

Fig. 23. PMD versus twist rate characteristics – IPHT 282b4.

was missing or modified. This difference deserves further investigation.

8.2. Comparisons

Fibers shared similar characteristics of PMD reduction with twist, but with a different sensitivity: twist rates required for a 50% PMD reduction were 133 rev/m for IPHT 252b5 and 14 rev/m for IPHT 282b4, respectively. Test on IPHT 252b5 demonstrated PMD reduction independent of twist direction, as expected for fibers drawn without spinning from a preform made of straight rods and tubes.

Plots in logarithmic scale (Figs. 24 and 25) indicate that DGD and PMD reduction follows the formula:

$$DGD = \frac{DGD_0}{1 + \left(\frac{\gamma}{\gamma_{th}}\right)^x},$$

where DGD_0 is the DGD of untwisted fiber, γ is the twist rate, γ_{th} is a threshold twist rate corresponding to 50% re-

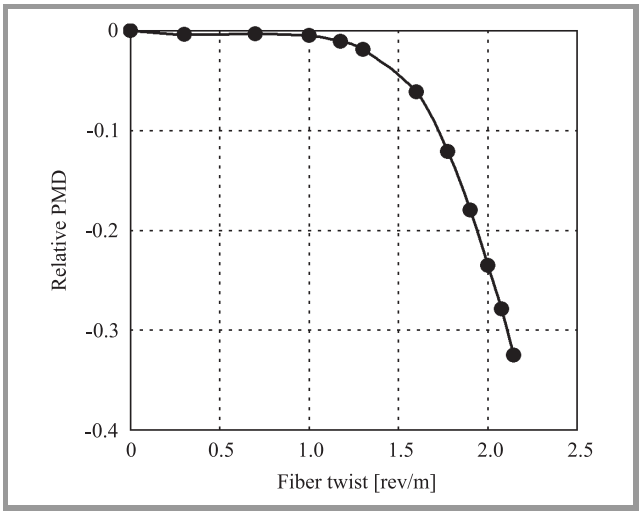

Fig. 24. PMD versus twist rate – IPHT 252b5 (logarithmic scale).

duction of DGD and x is a fixed exponent. While analysis presented in literature suggest either $x = 1$ [8] or $x = 2$ [7], our experimental data are best fitted by $x = 1.3$–1.7.

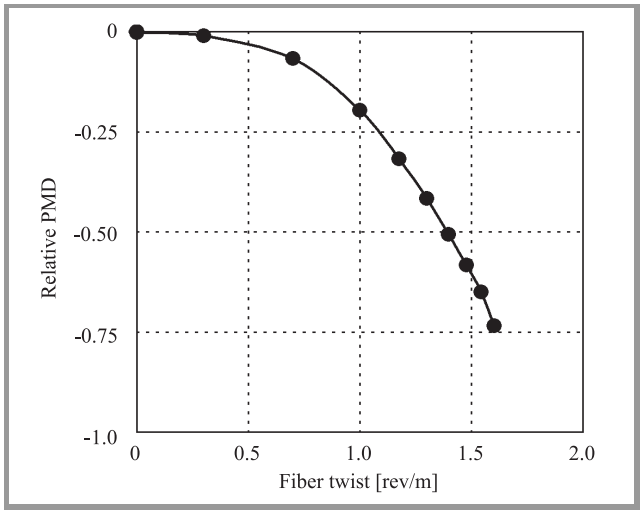

Fig. 25. PMD versus twist rate – IPHT 282b4 (logarithmic scale).

The DGD reduction with twist is wavelength-dependent: in IPHT 252b5 it was weaker with wavelength, in IPHT 282b4 stronger. In both samples, spectral distribution of DGD was flattest in untwisted state.

9. Elasto-Optic Coefficient

When optical fiber is elongated, decrease of effective refractive index partly compensates for increase of transmission delay due to extra length. This effect is important for design of fiber strain sensors.
Fiber under test was suspended vertically between fixed and movable clamp; delay was monitored by sending signal modulated at 69.632 MHz and measuring signal phase (Fig. 26). Tests were performed on sample of IPHT 252b5 being 10.50 m long, with applied strain up to 0.62%.
Change in transmission delay in strained fiber was calculated from phase shift of signal received at the end of this fiber versus reference signal from generator:

$$\Delta t = \Delta\varphi / 360 f ,$$

where: Δt – change in transmission delay [s], $\Delta\varphi$ – phase shift [deg], f – modulation frequency [Hz].

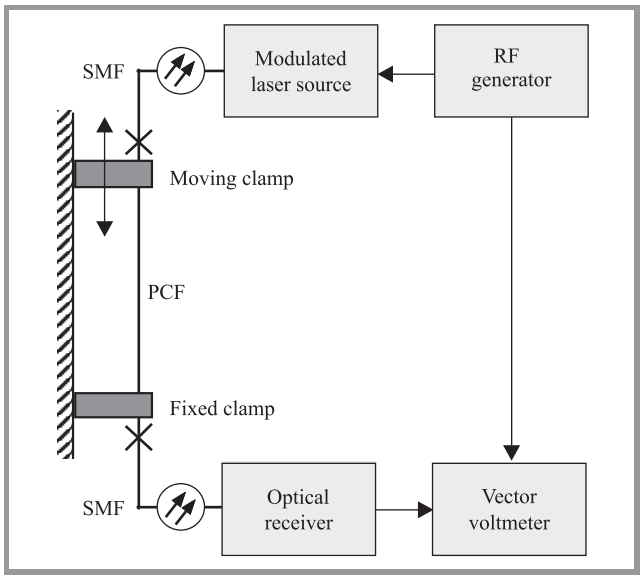

Fig. 26. Test setup for investigating elasto-optic coefficient of PCF.

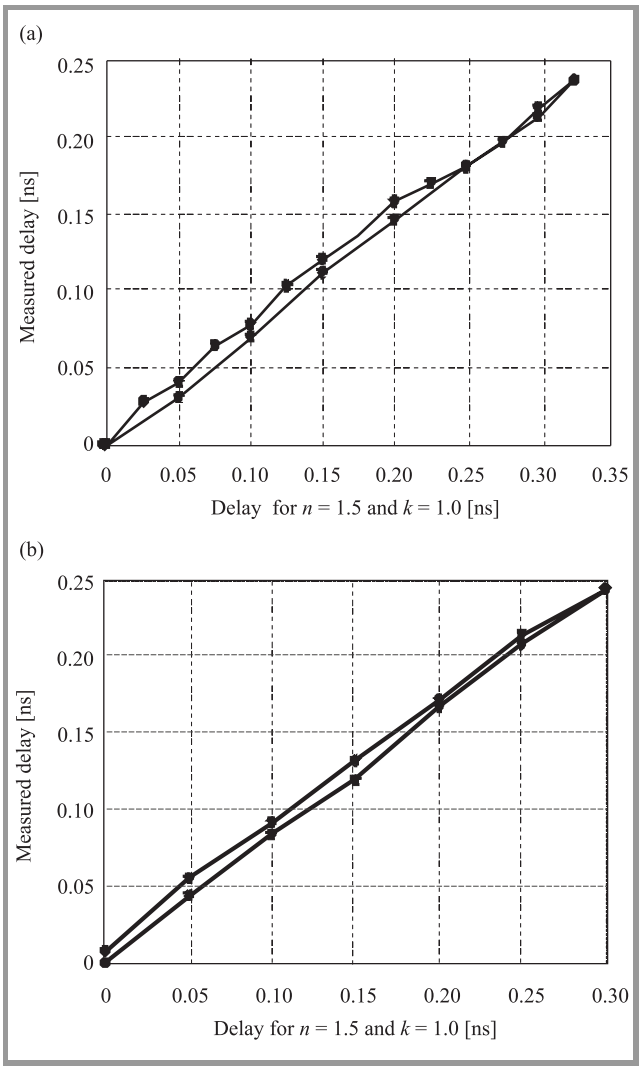

Fig. 27. Transmission delay introduced by fiber elongation versus effect of adding the same length of fiber, IPHT 252b5: (a) $\lambda = 1297$ nm, $k = 0.734$; (b) $\lambda = 1541$ nm, $k = 0.810$.

Measured change in transmission delay was compared to imaginary delay introduced by adding the same length of undisturbed fiber to transmission path. Their ratio is expressed as elasto-optic coefficient k:

$$k = c\Delta t / \Delta L n ,$$

where: c – speed of light in vacuum ($3 \cdot 10^8$ m/s), ΔL – fiber elongation [m], n – fiber refractive index (~ 1.50).

Figure 27 presents test data for IPHT 252b5 and two wavelengths. Values of k are little lower than for conventional SMF having $k \sim 0.80$ at 1300 nm, and similar as for dispersion-shifted fibers (DSF) and nonzero dispersion shifted fibers (NZ-DSF). This is quite surprising, considering small size and very strong doping (36% GeO_2) of core in this PCF.

10. Conlusions

Experiments on a two photonic crystal fibers of different designs have revealed properties unusual for conventional solid silica fibers, like strong PMD with very different temperature and twist dependence in each PCF tested. This proves such properties can be tailored to particular requirements by modifying PCF design. Moreover, PMD twist dependence does not exactly follow existing models.

Several other results are mostly consistent with previous reports, including:

- high polarization mode dispersion;
- very strong backscattering signal;
- high attenuation with spectral characteristics different from conventional fibers.

Such properties facilitate tests on short samples (0.5–100 m). In particular, twist dependence of PMD is extremely difficult to characterize in conventional single mode fibers due to long lengths required. Strong backscattering helps in OTDR measurements of short PCF lengths despite necessity to use short pulses. However, it makes OTDR measurements of splicing and coupling loss difficult and may be a limitation in applications where high return loss is required.

On the other hand, elasto-optic coefficient describing variations of transmission delay in axial strain conditions is similar in PCFs and conventional single mode fibers, defying predictions.

Fusion splicing of photonic crystal fibers to SMF, essential for measurements and in several applications can often be done with fairly low loss, but procedure must be individually tailored to each PCF.

Acknowledgements

The author is very grateful to our COST-299 partners, Kay Schuster and Jens Kobelke of IPHT Jena, Germany, for supplying fiber samples. The assistance of fellow NIT researchers, Tomasz Kossek and Tomasz Osuch during spectral loss measurements is kindly appreciated. Research presented in this paper has been financially supported by Polish Ministry of Science and Higher Education as special research project COST/39/2007.

References

[1] K. Borzycki, "Testing of highly doped and photonic crystal optical fibers", *J. Telecommun. Inform. Technol.*, no. 3, pp. 65–73, 2008.

[2] Corning SMF-28e Optical Fiber Product Information, Corning Inc., PI1344, Jan. 2005.

[3] Matched Cladding Single-Mode Fiber, OFS Fitel, fiber-106-0103, Jan. 2003.

[4] B. Edvold and L. Gruner-Nielsen, "New technique for reducing the splice loss to dispersion compensating fiber", in *Proc. ECOC-1996 Conf.*, Oslo, Norway, 1996, vol. 2, pp. 245–248.

[5] Y. Wang, H. Bartelt, S. Brueckner, J. Kobelke, M. Rothhardt, K. Mörl, W. Ecke, and R. Willsch, "Splicing Ge-doped photonic crystal fibers using commercial fusion splicer with default discharge parameters", *Opt. Expr.*, vol. 16, no. 10, pp. 7258–7263, 2008.

[6] R. E. Schuh, X. Shan, and A. S. Siddiqui, "Polarization mode dispersion in spun fibers with different linear birefringence and spinning parameters", *J. Lightw. Technol.*, vol. 16, no. 9, pp. 1583–1588, 1998.

[7] K. Borzycki, "Temperature dependence of polarization mode dispersion in tight-buffered optical fibers", *J. Telecommun. Inform. Technol.*, no. 1, pp. 56–66, 2008.

[8] J. Zhou, K. Tajima, K. Nakajima, K. Kurokawa, T. Matsui, Ch. Fukai, and I. Sankawa, "PMD suppression method for photonic crystal fiber", in *Proc. OFC-2005 Conf.*, Anaheim, USA, 2005, paper OTuA6.

[9] P. Lesiak and T. Woliński, "Simultaneous twist and longitudinal strain effects on polarization mode dispersion in highly birefringent fibers", *Opto-Electr. Rev.*, vol. 13, no. 2, pp. 183–186, 2005.

Krzysztof Borzycki was born in Warsaw, Poland, in 1959. He received the M.Sc. degree in electrical engineering from Warsaw University of Technology in 1982 and a Ph.D. degree in communications engineering from National Institute of Telecommunications (NIT), Warsaw in 2006. He has been with NIT since 1982, working on fusion splicing, optical transmission systems, measurement methods and test equipment for optical networks, as well as standardization and testing of optical fiber cables and DWDM systems. Other activities included being a lecturer and instructor in fiber optics and technical advisor to Polish cable industry. He has also been with Ericsson AB research laboratories in Stockholm, Sweden, working on development and testing of DWDM systems between 2001 and 2002. He has been active in several European projects since 2003, including Network of Excellence in Micro-Optics (NEMO) and COST Actions 270, 291 and 299. This included research on PMD in cables operating in extreme environments, and testing of specialty fibers. Dr. Borzycki is an author or co-author of 1 book, 2 Polish patents and 45 scientific papers in the field of optical fiber communications, optical fibers and measurements in optical networks, as well as one of "Journal of Telecommunications and Information Technology" editors.

e-mail: k.borzycki@itl.waw.pl
National Institute of Telecommunications
Szachowa st 1
04-894 Warsaw, Poland